Chapter 10
Frequency Detuning Control by Doppler Shift

Christian Holden, Dominik A. Breu, and Thor I. Fossen

10.1 Introduction

Control of parametric roll resonance has attracted considerable research in recent years [1, 7–11, 13–15, 18, 19]. The proposed control methods can roughly be categorized as *direct* or *indirect* methods. The direct methods are aimed at directly controlling the roll motion by generating an opposing roll moment, as seen in [11, 19]. Indirect strategies attempt to violate the empirical conditions necessary for the onset of parametric roll resonance, as seen in [1, 14, 15, 18]. A hybrid approach, doing both at the same time, is also possible, as seen in [7–9].

In this work, we consider the indirect approach to control parametrically excited roll motions. A simple model for parametric roll resonance is the *Mathieu equation*:

$$m_{44}\ddot{\phi} + d_{44}\dot{\phi} + \left[k_{44} + k_{\phi t}\cos(\omega_e t + \alpha_\phi)\right]\phi = 0,$$

where m_{44} is the sum of the moment of inertia and the added moment of inertia in roll, d_{44} the linear hydrodynamic damping coefficient, k_{44} the linear restoring moment coefficient and $k_{\phi t}$ the amplitude of its change, ω_e the encounter frequency, and α_ϕ a phase angle. All the parameters are considered constant.

It is known from [17] that such a system parametrically resonates at $\omega_e \approx 2\sqrt{k_{44}/m_{44}}$ (an encounter frequency of twice the natural roll frequency). The

C. Holden (✉) • D.A. Breu
Centre for Ships and Ocean Structures, Norwegian University of Science and Technology, NO-7491 Trondheim, Norway
e-mail: c.holden@ieee.org; breu@itk.ntnu.no

T.I. Fossen
Department of Engineering Cybernetics, Norwegian University of Science and Technology, NO-7491 Trondheim, Norway

Centre for Ships and Ocean Structures, Norwegian University of Science and Technology, NO-7491 Trondheim, Norway
e-mail: fossen@ieee.org

T.I. Fossen and H. Nijmeijer (eds.), *Parametric Resonance in Dynamical Systems*,
DOI 10.1007/978-1-4614-1043-0_10,

encounter frequency ω_e is the Doppler-shifted frequency of the waves as seen from the ship. As the frequency is Doppler-shifted, it can be changed by changing the ship's speed.

The main purpose of this chapter is to show that it is feasible to control parametric roll resonance by changing the encounter frequency to violate the condition $\omega_e \approx 2\sqrt{k_{44}/m_{44}}$. We call this frequency detuning.

As shown in Chap. 9, Mathieu-type equations are not valid for non-constant ω_e. To design and analyze the control system, we therefore use the simplified, 1-DOF model (9.39) developed in Sect. 9.5, allowing the ship's forward speed to change, but only slowly. For ships susceptible to parametric roll – many of which are large [2, 4–6] – this is not an unreasonable assumption.

Based on the 1-DOF roll model (9.39) in Sect. 9.5, we propose a simple controller based on a linear change of the encounter frequency, achieved by variation of the ship's forward speed. We then prove mathematically that the proposed controller is able to drive the ship out of parametric resonance, driving the roll motion to zero. It is worth noting that the controller is in fact simple enough that a human helmsman can perform the necessary control action, rendering a speed controller unnecessary.

The controller is tested with the simplified 1-DOF model (9.39) and the full 6-DOF model presented in Sect. 9.2.2, and is shown to work as expected in both cases.

The rest of this chapter is organized as follows. Section 10.2 lists nomenclature. Section 10.3 briefly summarizes the model used. The controller is derived and its theoretical properties are proven in Sect. 10.4. Its performance in simulation is shown in Sect. 10.5. Section 10.6 contains the conclusion. A short appendix contains the proof of a lemma used in the proof of the controller's performance.

10.2 Nomenclature

In this chapter, the following parameters are used:

$\mathbf{v}^b = [v_1^b, v_2^b, v_3^b]^\top$	The linear velocity of the ship observed in a reference frame attached to the ship.
$\boldsymbol{\omega}^b = [\omega_1^b, \omega_2^b, \omega_3^b]^\top$	The angular velocity of the ship observed in a reference frame attached to the ship.
$\mathbf{v}^n = [v_1^n, v_2^n, v_3^n]^\top$	The linear velocity of the ship observed in an (assumed inertial) reference frame attached to the mean ocean surface.
$\boldsymbol{\omega}^n = [\omega_1^n, \omega_2^n, \omega_3^n]^\top$	The angular velocity of the ship observed in an (assumed inertial) reference frame attached to the mean ocean surface.
$\mathbf{R}$	A rotation matrix rotating vectors from the body-fixed to the inertial frame.
$\boldsymbol{\Theta} = [\phi, \theta, \psi]^\top$	The roll–pitch–yaw Euler angles.
$m_{44} > 0$	The total moment of inertia in roll; the sum of the rigid-body moment of inertia in roll and the added moment of inertia in roll.
$d_{44} > 0$	The linear damping coefficient in roll.

$k_{44} > 0$	The linear restoring coefficient in roll.
$k_{\phi t} > 0$	The amplitude of the time-varying change in the linear restoring coefficient in roll.
$\omega_{\mathrm{e}}(t)$	The time-varying encounter frequency; the Doppler-shifted frequency of the waves as seen from the ship.
α_ϕ	The phase of the time-varying change in the linear restoring coefficient in roll.
$k_{\phi^3} > 0$	The cubic restoring coefficient in roll.
ω_0	The frequency of the waves as seen by an observer in an (assumed inertial) frame attached to the mean ocean surface.
k_{w}	The wave number as seen by an observer in an (assumed inertial) frame attached to the mean ocean surface.
$u = \dot{\omega}_{\mathrm{e}}$	The control input.
ε	A control parameter.
t	Time.
t_0	The start time.
t_1	The controller is turned on at time $t = t_1$.
t_2	The controller is turned off at time $t = t_2$.
$\omega_{\mathrm{e},0} = \omega_{\mathrm{e}}(t_0)$	The initial value of the encounter frequency.
$\omega_{\mathrm{e},1} = \omega_{\mathrm{e}}(t \geq t_2)$	The final value of the encounter frequency.
$\bar{\alpha}_\phi$	The phase of the time-varying change in the linear restoring coefficient in roll at time $t \geq t_2$.
γ	The normalized damping ratio.
κ	The normalized linear restoring coefficient.
ι	The normalized change in the linear restoring coefficient.
α	The normalized cubic restoring coefficient.
T	Normalized time (fast).
$\bar{t}$	Normalized time (slow).
σ	The detuning parameter.
$a(\bar{t})$	The (slowly) time-varying amplitude of the steady-state roll motion; $\phi \approx a(\bar{t})\cos(T - \beta(\bar{t})/2)$ for $t \geq t_2$.
$\beta(\bar{t})$	The (slowly) time-varying phase of the steady-state roll motion; $\phi \approx a(\bar{t})\cos(T - \beta(\bar{t})/2)$ for $t \geq t_2$.

10.3 Roll Model for Non-Constant Speed

As previously mentioned, we use no direct actuation in roll; instead, we are changing ω_{e} (by changing the forward speed) to detune the encounter frequency and thus violate a necessary condition for the existence of parametric roll resonance.

We make the following assumptions:

A 10.1. The ship is traveling in head or stern seas.

A 10.2. The waves are planar, standing, and sinusoidal, with frequency ω_0 and wave number k_{w}.

A 10.3. The ship is changing speed only slowly.
A 10.4. The ship's sway and heave velocities are small.
A 10.5. The ship's pitch angle is small.

The ship is traveling with linear and angular velocities

$$\mathbf{v}^b = [v_1^b, v_2^b, v_3^b]^\top \in \mathbb{R}^3 \tag{10.1}$$

$$\boldsymbol{\omega}^b = [\omega_1^b, \omega_2^b, \omega_3^b]^\top \in \mathbb{R}^3 \tag{10.2}$$

as seen from the ship. For an observer standing on the mean ocean surface, the ship will appear to have linear and angular velocities

$$\mathbf{v}^n = \mathbf{R}\mathbf{v}^b = [v_1^n, v_2^n, v_3^n]^\top \in \mathbb{R}^3 \tag{10.3}$$

$$\boldsymbol{\omega}^n = \mathbf{R}\boldsymbol{\omega}^b = [\omega_1^n, \omega_2^n, \omega_3^n]^\top \in \mathbb{R}^3, \tag{10.4}$$

where $\mathbf{R}$ is a rotation matrix given by:

$$\mathbf{R}(\boldsymbol{\Theta}) = \begin{bmatrix} c\theta c\psi & s\phi s\theta c\psi - c\phi s\psi & c\phi s\theta c\psi + s\phi s\psi \\ c\theta s\psi & s\phi s\theta s\psi + c\phi c\psi & c\phi s\theta s\psi - s\phi c\psi \\ -s\theta & s\phi c\theta & c\phi c\theta \end{bmatrix}, \tag{10.5}$$

where $c\cdot = \cos(\cdot)$, $s\cdot = \sin(\cdot)$ and $\boldsymbol{\Theta} = [\phi, \theta, \psi]^\top$ are the roll, pitch, and yaw angles as defined in [3], see also Chap. 9.

To analyze the effects of speed changes, we need a model that is valid for time-varying speed. As discussed in Chap. 9, the commonly used Mathieu equation is not adequate in this case. We thus use the 1-DOF model (9.39) of Sect. 9.5, given by

$$m_{44}\ddot{\phi} + d_{44}\dot{\phi} + \left[k_{44} + k_{\phi t}\cos\left(\int_{t_0}^{t} \omega_\mathrm{e}(t)\,\mathrm{d}\tau + \alpha_\phi\right)\right]\phi + k_{\phi^3}\phi^3 = 0, \tag{10.6}$$

where ϕ is the roll angle, m_{44} the sum of the rigid-body moment of inertia about the x-axis and the added moment of inertia in roll, d_{44} the linear hydrodynamic damping, k_{44} the linear restoring moment coefficient, $k_{\phi t}$ the amplitude of its change, and k_{ϕ^3} the cubic restoring force coefficient. These parameters are constant.

We note that the natural frequency of ϕ is $\omega_\phi \triangleq \sqrt{k_{44}/m_{44}}$. From Chap. 9, we have that the encounter frequency ω_e is given by:

$$\omega_\mathrm{e} = \omega_0 - k_\mathrm{w} v_1^n = \omega_0 - k_\mathrm{w}[1,0,0]\mathbf{R}\mathbf{v}^b\,. \tag{10.7}$$

The encounter frequency is the frequency of the waves as seen from the ship. Due to the Doppler effect, this is not the same as the frequency of the waves seen by a stationary observer, ω_0. For a ship traveling at constant velocity, ω_e is constant and the Mathieu equation can be used to describe the ship's behavior, see Chap. 9.

If the ship is nonrotating (i.e., $\boldsymbol{\omega}^b \equiv \mathbf{0}$), then

$$\begin{aligned}\dot{\omega}_\mathrm{e} &= -k_\mathrm{w}[1,0,0]\mathbf{R}\dot{\mathbf{v}}^b \approx -k_\mathrm{w}\mathbf{e}_x^\top \mathbf{R}[\dot{v}_1^b,0,0]^\top \\ &\approx -k_\mathrm{w}\dot{v}_1^b\cos(\theta)\cos(\psi) \approx -k_\mathrm{w}\dot{v}_1^b\cos(\psi) \end{aligned} \tag{10.8}$$

by the assumption of small sway velocity, yaw rate, and pitch angle. The ship is assumed to be sailing in head or stern seas, that is, $\cos(\psi) = 1$ (head seas) or $\cos(\psi) = -1$ (stern seas).

We can set $\dot{v}_1^b$ directly; this is the forward acceleration and can be changed by increasing or decreasing throttle. It will, however, be limited, so we take it to satisfy $|\dot{v}_1^b| \leq \dot{v}_{1,\max}^b$. Thus, we take $u \triangleq \dot{\omega}_\mathrm{e}$ to be the control input, satisfying

$$|u| = |\dot{\omega}_\mathrm{e}| \leq u_{\max} = |k_\mathrm{w}|\dot{v}_{1,\max}^b \,. \tag{10.9}$$

Note that the assumption that the forward speed changes only slowly implies that $v_{1,\max}^b$ is quite small. The assumption of slow speed change is a necessity to derive the model (10.6), as detailed in Sect. 9.5.

As we can see from the above equation, $u_{\max}$ depends on the size of $\dot{v}_{1,\max}^b$ and k_w. For the type of large, slow vessels that are susceptible to parametric roll, $\dot{v}_{1,\max}^b$ is likely to have quite a low value. For ships to parametrically resonate, the wave length has to be rather long, or $k_{\phi t}$ will be too small [12]. A long wave length implies a small k_w, since $|k_\mathrm{w}| = 2\pi/\lambda$ if λ is the wave length. Thus $u_{\max}$ is quite small.

10.4 Control Design

The control objective is to design u such that the origin of the roll system (10.6) is (at least) asymptotically stable. Choosing a $\dot{v}_1^b$ so that $\dot{\omega}_\mathrm{e}$ is equal to the desired u is a control allocation problem.[1]

10.4.1 Control Principle

The basic control principle is to (slowly) change the encounter frequency from an undesired value $\omega_{\mathrm{e},0}$ to a desired value $\omega_{\mathrm{e},1}$. We tentatively choose the controller

[1] It is also possible to change ω_e by changing course (i.e., changing ψ). This will have the unwanted side effect that the ship will now be directly excited by waves (i.e., there will be an external force on the right-hand side of (10.6) proportional to the wave amplitude), which may also result in relatively large roll amplitude in the type of seas that give rise to parametric resonance. Changing ψ to change the encounter frequency is not investigated in this work.

$$u(t) = \begin{cases} 0 & \forall \quad t \in [t_0, t_1] \\ \varepsilon & \forall \quad t \in [t_1, t_2] \\ 0 & \forall \quad t \in [t_2, \infty) \end{cases} \tag{10.10}$$

for some small constant ε, with $t_2 \geq t_1 \geq t_0$. The initial time is t_0.

If $\omega_e(t_0) = \omega_{e,0}$, then

$$\omega_e(t) = \int_{t_0}^{t} u(\tau)\, \mathrm{d}\tau + \omega_{e,0} = \begin{cases} \omega_{e,0} & \forall \quad t \in [t_0, t_1] \\ \omega_{e,0} + \varepsilon(t - t_1) & \forall \quad t \in [t_1, t_2] \\ \omega_{e,1} & \forall \quad t \in [t_2, \infty) \end{cases}, \tag{10.11}$$

where $\omega_{e,1} = \omega_{e,0} + \varepsilon(t_2 - t_1)$. This gives

$$\int_{t_0}^{t} \omega_e(\tau)\, \mathrm{d}\tau = \begin{cases} \omega_{e,0}(t - t_0) & \forall \quad t \in [t_0, t_1] \\ \omega_{e,0}(t - t_0) + \frac{1}{2}\varepsilon(t - t_1)^2 & \forall \quad t \in [t_1, t_2] \\ \omega_{e,1}(t - t_2) + \omega_{e,0}(t_2 - t_0) + \frac{1}{2}\varepsilon(t_2 - t_1)^2 & \forall \quad t \in [t_2, \infty) \end{cases}. \tag{10.12}$$

If $\cos(\psi) \equiv \pm 1$ and $v_2^b = v_3^b = \theta = 0$, then $\omega_e(t) = \omega_0 - k_w v_1^b \cos(\psi)$ and the encounter frequency of (10.11) can then be achieved with a surge velocity of

$$v_1^b = \frac{\omega_0 - \omega_e(t)}{k_w \cos(\psi)} = \frac{1}{k_w \cos(\psi)} \begin{cases} \omega_0 - \omega_{e,0} & \forall \quad t \in [t_0, t_1] \\ \omega_0 - \omega_{e,0} - \varepsilon(t - t_1) & \forall \quad t \in [t_1, t_2] \\ \omega_0 - \omega_{e,1} & \forall \quad t \in [t_2, \infty) \end{cases}. \tag{10.13}$$

Proving that the controller (10.10) works is done in two steps: First, ensuring that there exists a (unique finite) solution of (10.6) at $t = t_2$. This step is done in the Appendix. Secondly, we need to prove that if $\omega_e(t) \equiv \omega_{e,1}\ \forall\, t \geq t_2$, then the solution to the initial value problem

$$\begin{aligned} m_{44}\ddot{\phi} + d_{44}\dot{\phi} + \left[k_{44} + k_{\phi t}\cos\left(\omega_{e,1}t + \bar{\alpha}_\phi\right)\right]\phi + k_{\phi^3}\phi^3 = 0\,, \\ \phi(t_2) = \phi_2, \dot{\phi}(t_2) = \dot{\phi}_2\,, \end{aligned} \tag{10.14}$$

where

$$\bar{\alpha}_\phi \triangleq \alpha_\phi - \omega_{e,1}t_2 + \omega_{e,0}(t_2 - t_0) + \frac{1}{2}\varepsilon(t_2 - t_1)^2$$

is a constant, goes to zero for all ϕ_2, $\dot{\phi}_2$.

10.4.2 The System in the Time Interval $t \in [t_2, \infty)$

From the results in the Appendix, we know that there exists a unique finite solution to (10.6), valid at $t = t_2$. From $t \geq t_2$, the trajectories of the system will be the solution to the initial value problem (10.14).

From [17], we know that there are parameter values of $\omega_{e,1}$ which ensure that the trajectories of the system (10.14) go to zero. If we assume that $\omega_{e,0} \approx 2\omega_\phi$ (where parametric resonance of (10.6) is known to occur), we can find theoretical values for the regions of stability from the approximate methods of [17].

Theorem 10.1 (Main result). *Assuming that d_{44} is not very large, the behavior of (10.14) can be categorized into three different categories, depending on the value of $\omega_{e,1}$:*

- *If $0 \leq \omega_{e,1} \leq \underline{\omega}_e$, then the origin of (10.14) is globally attractive.*
- *If $\underline{\omega}_e < \omega_{e,1} \leq \overline{\omega}_e$, then the origin of (10.14) is unstable, and there exists a high-amplitude, stable limit cycle. All trajectories of (10.14) converge to this limit cycle, with the exception of those starting in the origin.*
- *If $\omega_{e,1} > \overline{\omega}_e$, then the origin of (10.14) is locally stable, there exists a high-amplitude, stable limit cycle, and a slightly lower-amplitude, unstable limit cycle.*

$\underline{\omega}_e$ and $\overline{\omega}_e$ are the solutions to the equations

$$\sqrt{1 - \frac{d_{44}^2 \underline{\omega}_e^2}{k_{\phi t}^2}} - \frac{m_{44}\underline{\omega}_e^2}{k_{\phi t}} \left(2\sqrt{\frac{k_{44}}{m_{44}\underline{\omega}_e}} - 1 \right) = 0 \tag{10.15}$$

$$\sqrt{1 - \frac{d_{44}^2 \overline{\omega}_e^2}{k_{\phi t}^2}} + \frac{m_{44}\overline{\omega}_e^2}{k_{\phi t}} \left(2\sqrt{\frac{k_{44}}{m_{44}\overline{\omega}_e}} - 1 \right) = 0\,. \tag{10.16}$$

If d_{44} is very large, then all solutions to the initial value problem (10.14) go to zero.

In this theorem, asymptotic stability of limit cycles follows the definition of [16, Definition 8.1].

Proof. To simplify the analysis, we define the alternative dimensionless time scale

$$T \triangleq \frac{1}{2}\omega_{e,1} t + \bar{\alpha}_\phi \tag{10.17}$$

giving

$$\frac{\mathrm{d}}{\mathrm{d}t} = \frac{1}{2}\omega_{e,1}\frac{\mathrm{d}}{\mathrm{d}T}$$
$$\frac{\mathrm{d}^2}{\mathrm{d}t^2} = \frac{1}{4}\omega_{e,1}^2\frac{\mathrm{d}}{\mathrm{d}T^2}\,.$$

Using primes to indicate derivatives with respect to T, we rewrite the system (10.14) as:

$$\phi'' + 2\imath\gamma\phi' + [\kappa + 2\imath\cos(2T)]\,\phi + \alpha\imath\phi^3 = 0, \tag{10.18}$$

where

$$\iota = \frac{2k_{\phi t}}{m_{44}\omega_{\mathrm{e},1}^2},$$

$$\gamma = \frac{d_{44}\omega_{\mathrm{e},1}}{2k_{\phi t}},$$

$$\kappa = \frac{4k_{44}}{m_{44}\omega_{\mathrm{e},1}},$$

$$\alpha = \frac{2k_{\phi^3}}{k_{\phi t}},$$

are all positive dimensionless parameters. It is assumed that ι is small.

Equation (10.18) is known to parametrically resonate if $\kappa \approx 1$ (i.e., $\omega_{\mathrm{e},0} \approx 2\omega_\phi$; the encounter frequency is twice the natural roll frequency).

Using an $O(\iota)$ (big O notation) approximation to the solution of (10.18), [17] derives a solution using the method of multiple scales (see [17]) given by:

$$\phi = a\cos(T - \beta/2) + O(\iota), \tag{10.19}$$

where a and β are slowly time-varying.

Defining an alternative (also dimensionless) time scale

$$\bar{t} = \iota T \tag{10.20}$$

(which is slowly varying) and letting

$$\sqrt{\kappa} = 1 - \iota\sigma \tag{10.21}$$

(with σ representing the nearness of κ to unity, and thus the system to parametric resonance), a and β satisfy the (nonlinear homogenous ordinary) differential equations

$$\frac{\partial a}{\partial \bar{t}} = -\frac{a}{2\sqrt{\kappa}}\sin(\beta) - \gamma a \tag{10.22}$$

$$a\frac{\partial \beta}{\partial \bar{t}} = 2\sigma a - \frac{a}{\sqrt{\kappa}}\cos(\beta) - \frac{3\alpha}{4\sqrt{\kappa}}a^3\,. \tag{10.23}$$

The a–β system has equilibrium points (corresponding to a steady-state periodic motion of ϕ, i.e., a limit cycle) given by:

$$a = 0, \qquad \beta \text{ is arbitrary} \tag{10.24}$$

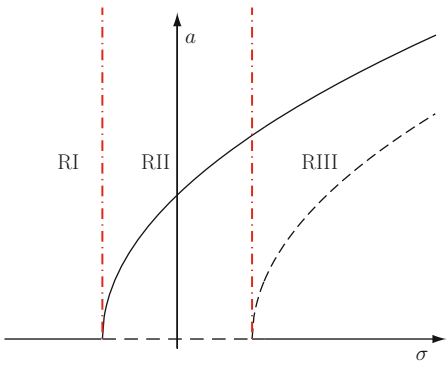

Fig. 10.1 Stability regions of (10.18), theoretical

(the trivial solution) and

$$\sin(\beta) = -2\sqrt{\kappa}\gamma, \quad \cos(\beta) = 2\sigma\sqrt{\kappa} - \frac{3\alpha}{4}a^2. \tag{10.25}$$

Since $\sqrt{\kappa} = 1 - \imath\sigma$, the non-trivial steady-state solution of ϕ has the amplitude

$$a^2 = \frac{8\sigma}{3\alpha} \pm \frac{4}{3\alpha}\sqrt{1-4\gamma^2}, \tag{10.26}$$

where only the positive root is relevant.

If $2\gamma > 1$, then (10.26) has no real roots and only the trivial steady-state solution exists. As this is equivalent to high damping, if $2\gamma > 1$, parametric resonance will not occur. (The origin of (10.18) is then globally attractive for all $\omega_{e,1}$).

If $2\gamma \leq 1$, then there is one real root of (10.26) if $2|\sigma| < \sqrt{1-4\gamma^2}$, and two if $2|\sigma| > \sqrt{1-4\gamma^2}$. The condition $2\sigma = -\sqrt{1-4\gamma^2}$ corresponds to (10.15) (giving $\underline{\omega}_e$) and $2\sigma = \sqrt{1-4\gamma^2}$ to (10.16) (giving $\overline{\omega}_e$).

Figure 10.1 illustrates the stability properties of (10.18) for the different cases. Dashed lines represent unstable equilibrium values of a for different values of σ, and solid lines stable equilibrium values.[2]

In Region RI, there is only the trivial solution. From [17], this is globally attractive.

In Region RII (where we have parametric resonance), the trivial solution is unstable, and there exists a large-amplitude steady-state solution, a limit cycle. Apart from the case where $\phi(t_2) = \dot{\phi}(t_2) = 0$, this limit cycle is globally attractive [17].

[2]It is worth noting that Fig. 10.1 bears strong similarity to a cross-section with the wave height kept constant of the simulation of the full 6-DOF model (9.8)–(9.9) of Sect. 9.2.2, except that in that chapter there is no evidence of the high-amplitude solutions of (10.18) in Region III. The stability regions indicated from simulating the 6-DOF model are shown in Fig. 10.2.

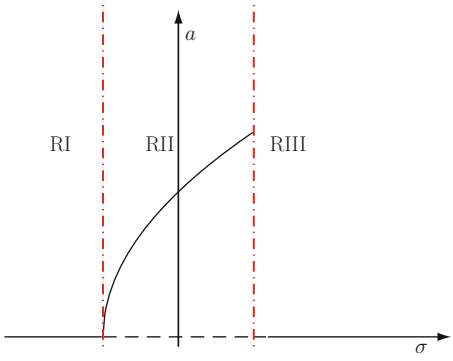

Fig. 10.2 Stability regions of the 6-DOF model (9.8)–(9.9) of Sect. 9.2.2, simulation

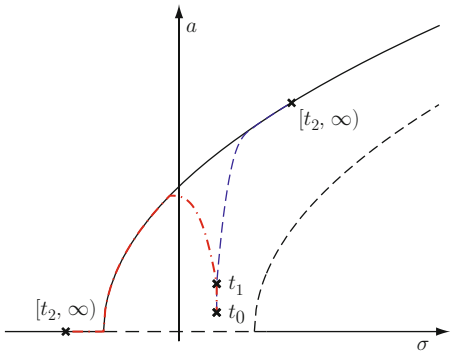

Fig. 10.3 Control of parametric roll resonance: Increasing versus decreasing the encounter frequency

Region RIII has three equilibrium values, and is somewhat more complicated. The value $a = 0$ (equivalent to $\phi = 0$) is (locally) asymptotically stable. However, there exist two limit cycles, one high-amplitude and one low-amplitude. The high-amplitude one is (locally) asymptotically stable, whereas the low-amplitude one is unstable. □

Based on the proof of Theorem 10.1, we conclude that it is possible that, if one increases ω_e so that $\omega_{e,1} \gg 2\omega_\phi$ (i.e., $\sigma \gg 0$), ϕ does not go to zero but instead to the high-amplitude limit cycle. If one instead decreases ω_e so that $\omega_{e,1} \ll 2\omega_\phi$ (i.e., $\sigma \ll 0$), ϕ will go to zero no matter how large $\phi(t_2)$ is. This is illustrated in Fig. 10.3.

This suggests that reducing the encounter frequency is the most sensible choice, and, in fact, the only option that can be guaranteed to work.

It is, however, worth noting that the analysis is based on a simplification of the ship dynamics. The high-amplitude limit cycle has not been observed in the simulations with the more physically accurate 6-DOF ship model (9.8)–(9.9) of Sect. 9.2.2. [8, 18] came to the opposite conclusion regarding speeding up versus slowing down. But bear in mind that in [8], the conclusion was largely predicated on the need to have sufficient speed for the fins (which were used in addition to speed change) to be effective.

None the less, decreasing the encounter frequency has another benefit: If we assume that σ starts at zero and slowly increases, trajectories will tend to go to a higher-amplitude limit cycle as the steady-state value of a increases with increasing σ in Region RII. However, if we instead decrease σ, trajectories will tend to go to a lower-amplitude limit cycle *even if we are still in parametric resonance*. This phenomenon has been observed in the simulations with the most accurate 6-DOF model (9.8)–(9.9) of Sect. 9.2.2, so there is reason to suspect that this holds true for real-world cases.

10.5 Simulation Results

To test the validity of the controller (10.10), we simulated the closed-loop system using both the simplified model (10.6) and the full 6-DOF model (9.8)–(9.9) of Sect. 9.2.2 in three different simulation scenarios. In all scenarios, we chose the initial conditions such that the ship was experiencing parametric roll resonance.

In accordance with the open-loop simulations in Chap. 9, a reduction of the frequency ratio to $\omega_{e,1}/\omega_\phi < 1.7$ will lead the ship out of the region where the ship is susceptible to parametric roll resonance.

We simulated three different scenarios:

1. *Slow* deceleration. The controller is turned on *after* parametric roll has already fully developed.
2. *Slow* deceleration. The controller is turned on *before* parametric roll has fully developed.
3. *Fast* deceleration. The controller is turned on *before* parametric roll has fully developed.

The simulation parameters (the same as those used in Chap. 9) are listed in Table 10.1. The control parameters are found in Tables 10.2–10.4. The simulation results are summarized in Table 10.5, and can be seen in Figs. 10.4–10.6.

Table 10.1 Simulation parameters

Quantity	Symbol	Value
Wave amplitude	ζ_0	2.5 m
Wave length	λ	281 m
Wave number	k_w	-0.0224 –
Natural roll frequency	ω_ϕ	0.343 rad/s
Modal wave frequency	ω_0	0.4684 rad/s
Simulation start time	t_0	0 s
	k_{44}	1.7533×10^9 kg m^2/s^2
Model parameters	$k_{\phi t}$	7.1373×10^8 kg m^2/s^2
(simplified roll equation)	α_ϕ	0.2741 rad
	k_{ϕ^3}	2.2627×10^9 kg m^2/s^2

Table 10.2 Control parameters, Scenario #1

Quantity	Symbol	Value
Control action	ε	-1.7889×10^{-4} rad/s^2
Maximum deceleration	$\dot{v}_{1,\max}$	0.008 m/s^2
Initial forward speed	$v_1(t_0)$	7.44 m/s
Initial encounter frequency	$\omega_{e,0}$	0.6346 rad/s
Final encounter frequency	$\omega_{e,1}$	0.5831 rad/s
Final forward speed	$v_1(t_2)$	5.14 m/s
Controller turned on	t_1	300 s
Controller turned off	t_2	588 s

Table 10.3 Control parameters, Scenario #2

Quantity	Symbol	Value
Control action	ε	-1.7889×10^{-4} rad/s^2
Maximum deceleration	$\dot{v}_{1,\max}$	0.008 m/s^2
Initial forward speed	$v_1(t_0)$	7.44 m/s
Initial encounter frequency	$\omega_{e,0}$	0.6346 rad/s
Final encounter frequency	$\omega_{e,1}$	0.5831 rad/s
Final forward speed	$v_1(t_2)$	5.14 m/s
Controller turned on	t_1	93 s
Controller turned off	t_2	381 s

Table 10.4 Control parameters, Scenario #3

Quantity	Symbol	Value
Control action	ε	-3.5778×10^{-4} rad/s^2
Maximum deceleration	$\dot{v}_{1,\max}$	0.016 m/s^2
Initial forward speed	$v_1(t_0)$	6.67 m/s
Initial encounter frequency	$\omega_{e,0}$	0.6174 rad/s
Final encounter frequency	$\omega_{e,1}$	0.5660 rad/s
Final forward speed	$v_1(t_2)$	4.37 m/s
Controller turned on	t_1	55 s
Controller turned off	t_2	199 s

Table 10.5 Simulation results, maximum roll angles

	Simplified 1-DOF model			Full 6-DOF model		
Scenarios	Uncontrolled	Controlled	Reduction	Uncontrolled	Controlled	Reduction
#1	25.34°	25.34°	0%	23.34°	23.34°	0%
#2	25.34°	22.40°	11.6%	23.34°	20.33°	9.0%
#3	23.57°	13.71°	41.8%	17.99°	4.83°	73.2%

Figure 10.4 shows the simulation results for the controlled system in comparison with the uncontrolled system for the first scenario. It is obvious from Fig. 10.4a that the ship is experiencing large roll amplitudes caused by parametric resonance. The frequency ratio is gradually decreased after 300 s (Fig. 10.4c), which causes the expected gradual reduction of the roll motion to zero.

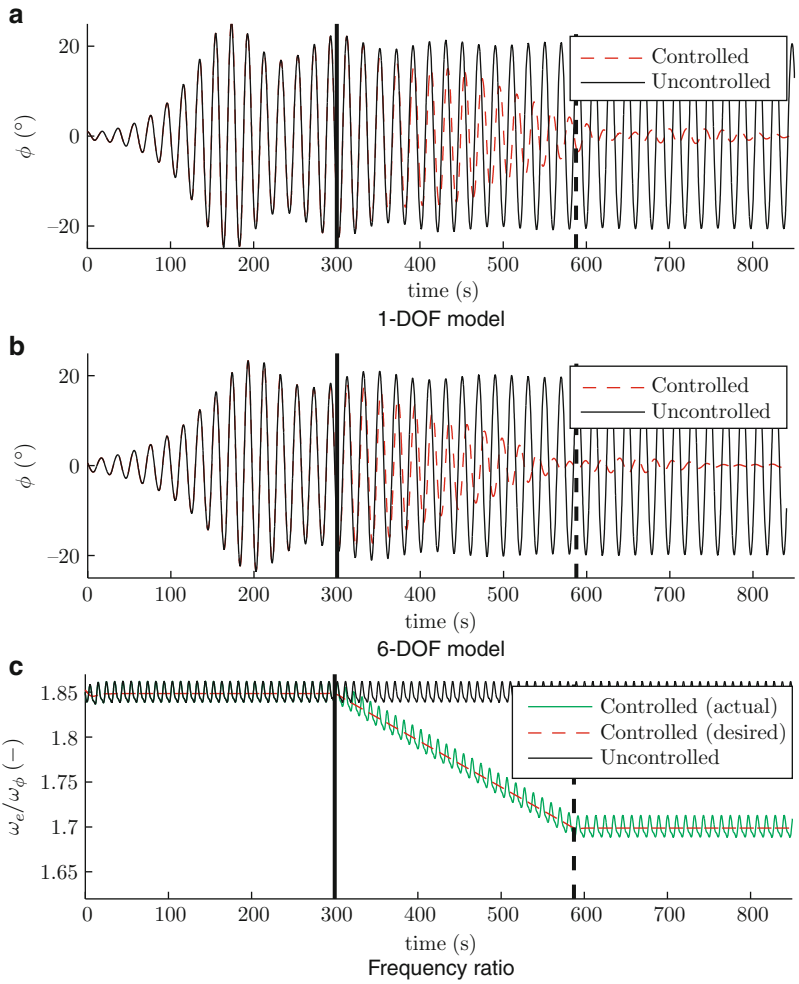

Fig. 10.4 Simulation results, Scenario #1

The simulation results with the full 6-DOF model (9.8)–(9.9) of Sect. 9.2.2 are shown in Fig. 10.4b. The controller works equally well with the more complex model.

Of course, since the controller is turned on only after parametric roll has fully developed, the maximum roll angle in Scenario #1 is the same for the controlled and uncontrolled cases. (The steady-state roll angle is zero as predicted.)

The simulation results of the second scenario are shown in Fig. 10.5. In this scenario, we reduce the encounter frequency when the roll angle is much lower than in the first scenario, early enough that parametric rolling has not yet fully developed (specifically, when the roll angle is about 5°). Figure 10.5 shows that both the simplified 1-DOF model and the full 6-DOF model behave similarly.

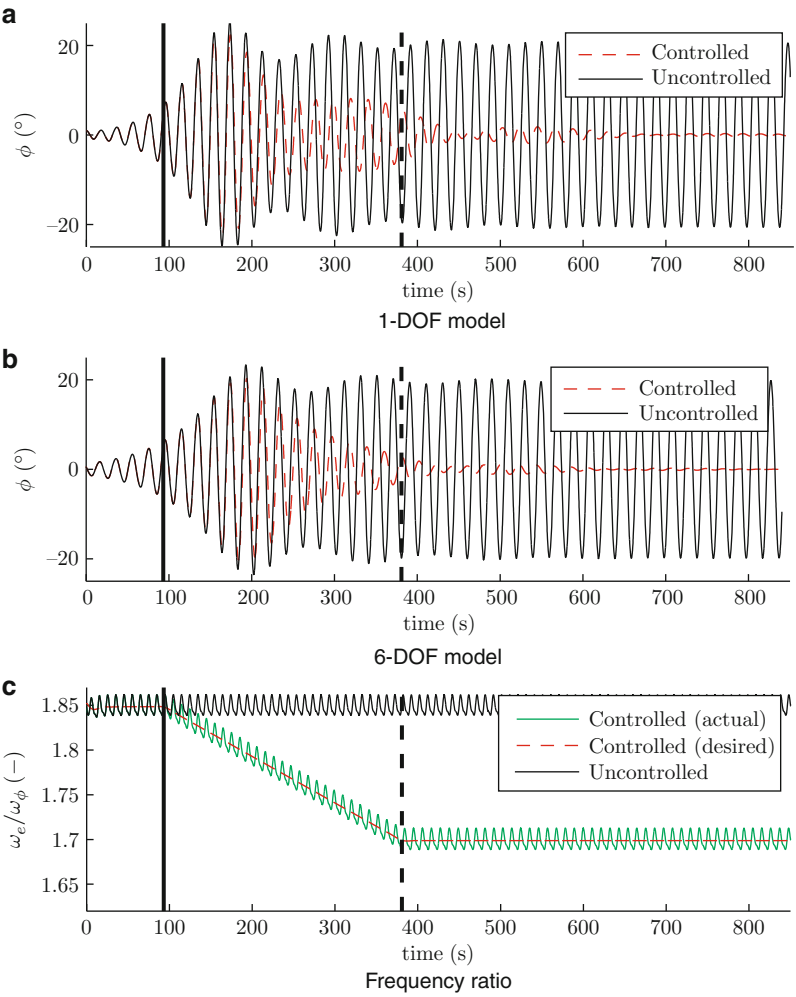

Fig. 10.5 Simulation results, Scenario #2

However, despite the controller being turned on when roll is only at 5°, the maximum roll angle is not greatly reduced compared to the uncontrolled case. This is simply because the ship is moving very slowly out of resonant condition. The steady-state roll angle is none the less zero, as predicted.

To get the ship to move out of resonant condition before the roll angle has reached dangerous levels requires, as it turned out, significantly faster deceleration than in Scenarios #1 and #2, even if the controller was turned on at a lower roll angle.

To this effect, we simulated Scenario #3. The controller is turned on early, at a time when the roll angle is about 2°. The ship is decelerating at twice the rate of Scenarios #1 and #2. Also, both the initial and final encounter frequencies are lower in Scenario #3 than in the two others. The results are plotted in Fig. 10.6.

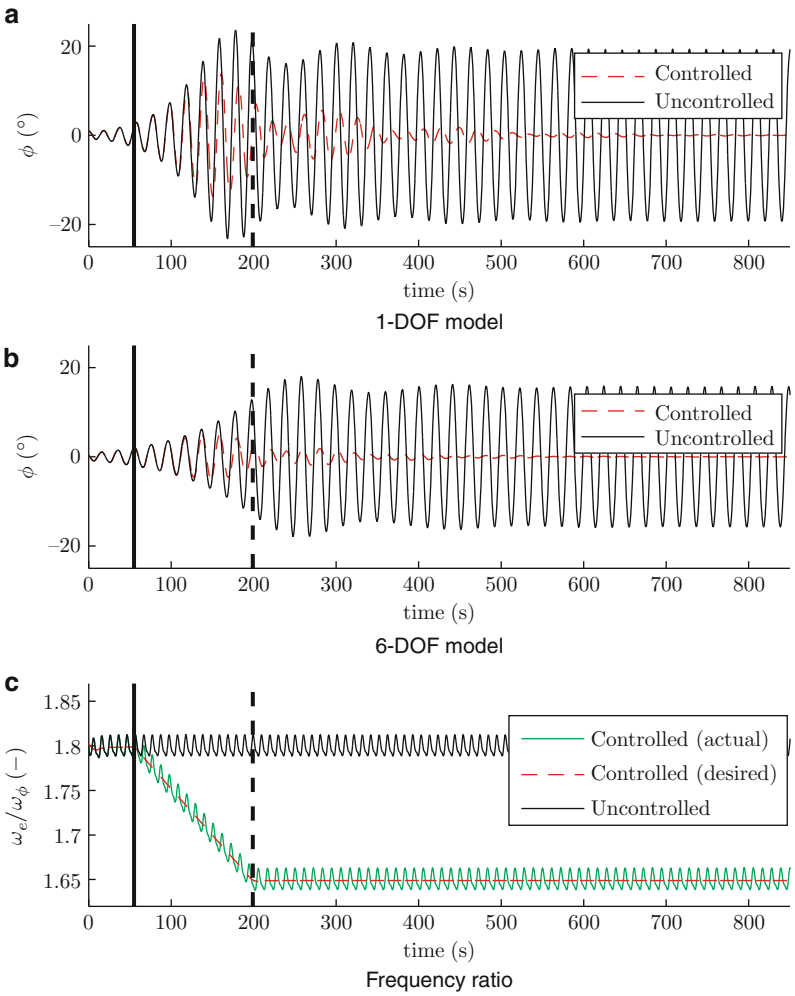

Fig. 10.6 Simulation results, Scenario #3

From Fig. 10.6, we see that the controller is capable of reducing the roll angle sufficiently fast such that the maximum roll angle is only from 1/2 (1-DOF model) to 1/4 (6-DOF model) of the maximum roll angle of the uncontrolled case. Interestingly, from Fig. 10.6 we see that the controller works significantly better for the full 6-DOF model than for the simplified 1-DOF model. In steady-state, the roll angle is zero, as expected.

From the simulation results, we see that the controller is capable of bringing the ship out of parametric resonance and – assuming sufficient deceleration capability – reduce the maximum roll angle significantly. It is also vital to turn on the controller as early as possible. The simulations confirm the theoretical derivations presented in Sect. 10.4.

How practical the controller is in a real-world scenario depends almost entirely on the ability of the captain (or the automated systems) to detect parametric resonance, and the ability of the ship to rapidly decelerate. If these capabilities are present, then the controller could prove useful. In the absence of one or both of these abilities, the practicality of the controller is limited, at least on its own. However, it might be possible to pair it with another control scheme such as fins as done in [7, 9], u-tanks (investigated on their own in Chap. 12), gyro stabilizers, or other active controllers.

10.6 Conclusions

A necessary, but not sufficient, condition for parametric resonance is that the frequency of the parametric excitation has certain values. For ships, this frequency can be changed (due to the Doppler effect) by changing the velocity. In this work, we have derived a controller for parametric roll resonance in ships that takes advantage of this and can drive the roll motion to zero. We call this frequency detuning control.

Based on the simplified 1-DOF roll model (9.39) developed in Sect. 9.5, we proposed a simple controller incorporating a linear change of the wave encounter frequency, accomplished by changing the forward speed of the ship. We showed mathematically and in simulations – using both the simplified model and the 6-DOF model (9.8)–(9.9) of Sect. 9.2.2 – that the proposed controller drives the roll motion to zero. The derived controller is so simple that it can be implemented by a helmsman, even without a speed controller on board.

However, while the controller drives the roll angle to zero, the transient behavior can be problematic. Even if the controller is turned on at a very early stage, the ship will have to be capable of a fairly rapid speed change to prevent high transient roll angles. Frequency detuning does have the advantage that it can easily be paired with direct actuation, such as the use of u-tanks, fins, or gyro stabilizers.

The effectiveness of the frequency detuning controller can be further increased by course changes in addition to speed changes to alter the encounter frequency. However, this can cause regular, directly induced roll excitation to become a problem, and was not investigated in this work.

Frequency detuning can be used for other parametrically resonating systems as long as it is possible to change the frequency of excitation. However, for most systems with the ability to change the frequency of excitation, one presumably also has the ability to change the amplitude of excitation. In that case, it is probably easier to do so. In practice, this limits the applicability of the proposed control scheme to a few systems, most notably those where the parametric resonance is induced by flow past a free-moving body.

Acknowledgements This work was funded by the Centre for Ships and Ocean Structures (CeSOS), NTNU, Norway, and the Norwegian Research Council.

Appendix

In this appendix, we prove the existence and uniqueness properties of (10.6).

From [17], we get the behavior of the system when ω_e is a constant, but not when it is changing. We need to guarantee a unique finite solution of (10.6) also for time-varying ω_e.

To prove the existence (and uniqueness) of the solution to (10.6), we will use the following theorem and lemma, repeated here for convenience:

Theorem 10.2 ([16, Theorem 3.3]). *Let $f(t,x)$ be piecewise continuous in t and locally Lipschitz in x for all $t \geq t_0$ and all x in a domain $D \subset \mathbb{R}^n$. Let W be a compact subset of D, $x_0 \in W$, and suppose it is known that every solution of*

$$\dot{x} = f(t,x), \qquad x(t_0) = x_0$$

lies entirely in W. Then there is a unique solution that is defined for all $t \geq t_0$.

Lemma 10.1 ([16, Lemma 3.2]). *If $f(t,x)$ and $\frac{\partial f}{\partial x}(t,x)$ are continuous on $[a,b] \times D$, for some domain $D \subset \mathbb{R}^n$, then f is locally Lipschitz in x on $[a,b] \times D$.*

If we take $x = [\phi, \dot{\phi}]^\top$, we can rewrite (10.6) as

$$\begin{aligned}
\dot{x} &= \begin{bmatrix} x_2 \\ -\frac{d_{44}}{m_{44}} x_2 - \frac{1}{m_{44}} \left[k_{44} + k_{\phi t} \cos\left(\int_{t_0}^{t} \omega_e(\tau)\, \mathrm{d}\tau + \alpha_\phi \right) \right] x_1 - \frac{k_{\phi^3}}{m_{44}} x_1^3 \end{bmatrix} = f(t,x) \\
&= \begin{bmatrix} 0 & 1 \\ -\frac{k_{44}}{m_{44}} & -\frac{d_{44}}{m_{44}} \end{bmatrix} x + \begin{bmatrix} 0 \\ -\frac{k_{\phi t}}{m_{44}} \cos\left(\int_{t_0}^{t} \omega_e(\tau)\, \mathrm{d}\tau + \alpha_\phi \right) x_1 - \frac{k_{\phi^3}}{m_{44}} x_1^3 \end{bmatrix} \\
&= Ax + g(t,x_1) \qquad (10.27)
\end{aligned}$$

with

$$\begin{aligned}
f(t,x) &\triangleq \begin{bmatrix} x_2 \\ -\frac{d_{44}}{m_{44}} x_2 - \frac{1}{m_{44}} \left[k_{44} + k_{\phi t} \cos\left(\int_{t_0}^{t} \omega_e(\tau)\, \mathrm{d}\tau + \alpha_\phi \right) \right] x_1 - \frac{k_{\phi^3}}{m_{44}} x_1^3 \end{bmatrix} \\
A &\triangleq \begin{bmatrix} 0 & 1 \\ -\frac{k_{44}}{m_{44}} & -\frac{d_{44}}{m_{44}} \end{bmatrix} \\
g(t,x_1) &\triangleq \begin{bmatrix} 0 \\ -\frac{k_{\phi t}}{m_{44}} \cos\left(\int_{t_0}^{t} \omega_e(\tau)\, \mathrm{d}\tau + \alpha_\phi \right) x_1 - \frac{k_{\phi^3}}{m_{44}} x_1^3 \end{bmatrix}.
\end{aligned}$$

Lemma 10.2. *There is a unique solution of (10.27) (and thus (10.6)) defined for all $t \geq t_0$.*

Proof. It is clear that $f(t,x)$ of (10.27) is continuous in x for all $x \in \mathbb{R}^2$. It is also continuous in t for all $t \geq t_0$, as long as $\omega_e(t)$ is piecewise continuous. Our choice of ω_e satisfies this.

The partial derivative of f with respect to x is given by:

$$\frac{\partial f}{\partial x}(t,x) = A - \begin{bmatrix} 0 & 0 \\ \frac{k_{\phi t}}{m_{44}} \cos\left(\int_{t_0}^{t} \omega_e(\tau)\, \mathrm{d}\tau + \alpha_\phi\right) + 3\frac{k_{\phi^3}}{m_{44}} x_1^2 & 0 \end{bmatrix} \tag{10.28}$$

which, by the same argument, is continuous in x for all $x \in \mathbb{R}^2$ and $t \geq t_0$. By [16, Lemma 3.2], f is therefore locally Lipschitz in x for all $t \geq t_0$ and all $x \in \mathbb{R}^2$. The first part of [16, Theorem 3.3] is then satisfied.

To prove that the trajectories of the system are bounded, we use the Lyapunov function candidate

$$V = \frac{1}{2} x^\top P x + \frac{1}{4}\left(1 + \frac{m_{44}}{d_{44}}\right) k_{\phi^3} x_1^4 \tag{10.29}$$

with

$$P = \begin{bmatrix} d_{44} + k_{44}\left(1 + \frac{m_{44}}{d_{44}}\right) & m_{44} \\ m_{44} & m_{44}\left(1 + \frac{m_{44}}{d_{44}}\right) \end{bmatrix} = P^\top > 0\,. \tag{10.30}$$

The time derivative of V along the trajectories of the system (10.27) is given by:

$$\begin{aligned} \dot{V} &= x^\top P\left(Ax + g(t,x)\right) + \left(1 + \frac{m_{44}}{d_{44}}\right) k_{\phi^3} x_1^3 x_2 \\ &= -\left(k_{44} + k_{\phi t} \cos\left(\int_{t_0}^{t} \omega_e(\tau)\, \mathrm{d}\tau + \alpha_\phi\right)\right) x_1^2 - d_{44} x_2^2 - k_{\phi^3} x_1^4 \\ &\quad - k_{\phi t} \cos\left(\int_{t_0}^{t} \omega_e(\tau)\, \mathrm{d}\tau + \alpha_\phi\right)\left(1 + \frac{m_{44}}{d_{44}}\right) x_1 x_2 \\ &\leq -\left(k_{44} - k_{\phi t}\right) x_1^2 - d_{44} x_2^2 - k_{\phi^3} x_1^4 + k_{\phi t}\left(1 + \frac{m_{44}}{d_{44}}\right) |x_1||x_2|\,. \end{aligned} \tag{10.31}$$

While $k_{44} > k_{\phi t}$, $\dot{V}$ is only negative definite for sufficiently small values of $k_{\phi t}$. If $k_{\phi t}$ *is* sufficiently small, then the origin of the system (10.27) would be globally uniformly exponentially stable, by [16, Theorem 4.10]. A priori we know that this is not the case; in parametric resonance, the origin is, in fact, unstable.

However, V can be used to prove that the trajectories of (10.27) are bounded.

For $|x_1| \geq \mu > 0 \Rightarrow \|x\| \geq \mu$ it holds that

$$\begin{aligned}\dot{V} &\leq -\left(k_{44} - k_{\phi t}\right) x_1^2 - d_{44} x_2^2 - k_{\phi^3} x_1^4 + k_{\phi t}\left(1 + \frac{m_{44}}{d_{44}}\right)|x_1||x_2| \\ &\leq -d_{44} x_2^2 - k_{\phi^3}\mu^2 x_1^2 + k_{\phi t}\left(1 + \frac{m_{44}}{d_{44}}\right)|x_1||x_2| \\ &= -(1-\delta) d_{44} x_2^2 - (1-\delta) k_{\phi^3}\mu^2 x_1^2 \\ &\quad + k_{\phi t}\left(1 + \frac{m_{44}}{d_{44}}\right)|x_1||x_2| - \delta d_{44} x_2^2 - \delta k_{\phi^3}\mu^2 x_1^2 \end{aligned} \tag{10.32}$$

for some $\delta \in (0,1)$. Furthermore, the term

$$k_{\phi t}\left(1 + \frac{m_{44}}{d_{44}}\right)|x_1||x_2| - \delta d_{44} x_2^2 - \delta k_{\phi^3}\mu^2 x_1^2$$

is negative semidefinite if

$$k_{\phi t}^2\left(1 + \frac{m_{44}}{d_{44}}\right)^2 \leq 4 d_{44}\delta^2 k_{\phi^3}\mu^2 \quad \Rightarrow \quad \mu \geq \frac{1}{2\delta\sqrt{d_{44} k_{\phi^3}}} k_{\phi t}\left(1 + \frac{m_{44}}{d_{44}}\right). \tag{10.33}$$

Therefore, for μ satisfying the above inequality,

$$\dot{V} \leq -(1-\delta) d_{44} x_2^2 - (1-\delta) k_{\phi^3}\mu^2 x_1^2 \tag{10.34}$$

which is negative definite. By [16, Theorem 4.18] the trajectories of (10.27) are bounded for any initial condition $x(t_0)$.

Therefore, the second condition of [16, Theorem 3.3] is satisfied, and there exists a unique solution of (10.27) (and thus (10.6)) that is defined for all $t \geq t_0$. □

References

1. Breu, D.A., Fossen, T.I.: Extremum seeking speed and heading control applied to parametric resonance. In: Proceeding of IFAC Conference on Control Applications in Marine Systems. Rostock, Germany (2010)
2. Carmel, S.M.: Study of parametric rolling event on a panamax container vessel. Journal of the Transportation Research Board **1963**, 56–63 (2006)
3. Fossen, T.I.: Handbook of Marine Craft Hydrodynamics and Motion Control. John Wiley & Sons, Ltd., Chichester, UK (2011)

4. France, W.N., Levadou, M., Treakle, T.W., Paulling, J.R., Michel, R.K., Moore, C.: An investigation of head-sea parametric rolling and its influence on container lashing systems. SNAME Annual Meeting, Orlando, Florida, USA (2001)
5. Francescutto, A.: An experimental investigation of parametric rolling in head waves. Journal of Offshore Mechanics and Arctic Engineering **123**, 65–69 (2001)
6. Francescutto, A., Bulian, G.: Nonlinear and stochastic aspects of parametric rolling modelling. In: Proceedings of 6th International Ship Stability Workshop. New York, USA (2002)
7. Galeazzi, R.: Autonomous supervision and control of parametric roll resonance. PhD thesis, Technical University of Denmark (2009)
8. Galeazzi, R., Blanke, M.: On the feasibility of stabilizing parametric roll with active bifurcation control. In: Proceedings of IFAC Conference on Control Applications in Marine Systems. Bol, Croatia (2007)
9. Galeazzi, R., Holden, C., Blanke, M., Fossen, T.I.: Stabilization of parametric roll resonance by combined speed and fin stabilizer control. In: Proceedings of European Control Conference. Budapest, Hungary (2009)
10. Galeazzi, R., Vidic-Perunovic, J., Blanke, M., Jensen, J.J.: Stability Analysis of the Parametric Roll Resonance under Non-constant Ship Speed In: Proceedings of ESDA2008, 9th Biennial ASME Conference on Engineering Systems Design and Analysis. Haifa, Israel (2008)
11. Holden, C., Galeazzi, R., Fossen, T.I., Perez, T.: Stabilization of parametric roll resonance with active u-tanks via lyapunov control design. In: Proceedings of European Control Conference. Budapest, Hungary (2009)
12. Holden, C., Galeazzi, R., Rodríguez, C.A., Perez, T., Fossen, T.I., Blanke, M., Neves, M.A.S.: Nonlinear container ship model for the study of parametric roll resonance. Modeling, Identification and Control **28**(4) (2007)
13. Holden, C., Perez, T., Fossen, T.I.: A lagrangian approach to nonlinear modeling of anti-roll tanks. Ocean Engineering **38**(2–3), 341–359 (2011)
14. Jensen, J.J., Pedersen, P.T., Vidic-Perunovic, J.: Estimation of parametric roll in stachastic seaway. In: Proceedings of IUTAM Symposium on Fluid-Structure Interaction in Ocean Engineering. Hamburg, Germany (2007)
15. Jensen, J.J., Vidic-Perunovic, J., Pedersen, P.T.: Influence of surge motion on the probability of parametric roll in a stationary sea state. In: Proceedings of 10th International Ship Stability Workshop. Hamburg, Germany (2007)
16. Khalil, H.: Nonlinear Systems, 3rd edn. Prentice Hall, Upper Saddle, New Jersey, USA (2002)
17. Nayfeh, A.H., Mook, D.T.: Nonlinear Oscillations. John Wiley & Sons, Inc., Weinheim, Germany (1995)
18. Ribeiro e Silva, S., Santos, T.A., Soares, C.G.: Parametrically excited roll in regular and irregular head seas. International Shipbuilding Progress **51**, 29–56 (2005)
19. Umeda, N., Hashimoto, H., Vassalos, D., Urano, S., Okou, K.: An investigation of different methods for the prevention of parametric rolling. Journal of Marine Science and Technology **13**, 16–23 (2008)